Nature and Significance of the Interactions between Amyloid Fibrils and Biological Polyelectrolytes†

Martino Calamai,‡ Janet R. Kumita,‡ John Mifsud,‡ Claudia Parrini,§ Matteo Ramazzotti,§ Giampietro Ramponi,§ Niccoló Taddei,§ Fabrizio Chiti,§ and Christopher M. Dobson*,‡

Department of Chemistry, University of Cambridge, Lensfield Road, Cambridge, CB2 1EW, U.K., and Dipartimento di Scienze Biochimiche, Università degli Studi di Firenze, Viale Morgagni 50, 50134, Firenze, Italy

Received May 29, 2006; Revised Manuscript Received August 16, 2006

ABSTRACT: Charged polyelectrolytes such as glycosaminoglycans and nucleic acids have frequently been found associated with the proteinaceous deposits in the tissues of patients with amyloid diseases. We have investigated the nature and generality of this phenomenon by studying the ability of different polyanions, including DNA, ATP, heparin, and heparan sulfate, to promote the aggregation of amyloidogenic proteins and to bind to the resulting aggregates. Preformed amyloid fibrils of human muscle acylphosphatase and human lysozyme, proteins with a net positive charge at physiological pH values, were found to bind tightly to the negatively charged DNA or ATP. The effects of the polyelectrolytes on the kinetics of aggregation were studied for acylphosphatase, and the presence of ATP, DNA, or heparin was found to increase its aggregation rate dramatically, with a degree dependent on the net charge and size of the polyanion. Magnesium or calcium ions were found to attenuate, and ultimately to suppress, these interactions, suggesting that they are electrostatic in nature. Moreover, heparin was found to stabilize the aggregated state of acylphosphatase through compensation of electrostatic repulsion. Noteworthy, differences in affinity between native and aggregated acylphosphatase with heparin suggest that amyloid fibrils can themselves behave as polyelectrolytes, interacting very strongly with other polyelectrolytes bearing the opposite charge. Within an in vivo context, the strengthening of the electrostatic interactions with other biological polyelectrolytes, as a consequence of protein misfolding and aggregation, could therefore result in depletion of essential molecular components and contribute to the known cytotoxicity of amyloid fibrils and their precursors.

Amyloid diseases are characterized by the deposition in a variety of tissues of specific proteins as aggregated species that share a distinctive fibrillar ultrastructure (*1*−*3*). Although amyloid deposits are predominantly proteinaceous, as demonstrated by Friedreich and Kekule in 1859 (*4*), careful examination of diseased tissues has revealed the presence of a significant quantity of polysaccharide species associated with the deposits. These polysaccharides belong to the glycosaminoglycan family (GAGs[1]) and are long unbranched chains of repeating disaccharide units. Among these species, heparan sulfate is the most common, being found in a variety of amyloid disorders including Alzheimer's disease, type II diabetes, light chain amyloidosis, and the prion related diseases (*5*−*7*). While direct binding of heparan sulfate or heparin, the hypersulfated form of heparan sulfate, to soluble amyloid precursor proteins has been established in many cases, the ability of these polymers to promote fibrillogenesis has been investigated for only a few peptides or proteins, such as the Aβ peptides (*8, 9*), tau (*10, 11*), α-synuclein (*12*), and β2-microglobulin (*13*).

GAGs are not, however, the only polyanions found to be associated with amyloid fibrils. In the brain tissue from victims of Alzheimer's disease, for example, nucleic acids have been detected in neurofibrillary tangles, intracellular inclusions primarily composed of the tau protein, as well as in senile plaques composed of the Aβ peptides (*14*). Moreover, it has been shown that RNA is able to stimulate the aggregation of tau (*11, 15*) and to induce the conversion of PrP^{C} to PrP^{Sc} (*16*), while DNA can promote fibril formation by α-synuclein (*17*). Interestingly, DNA can bind strongly after cell lysis to the amyloid-like Curli fibrils of *Escherichia coli* (*18*), and ATP has been found to promote the formation of fibrils of Aβ peptide and amylin (*19, 20*).

Despite the ubiquitous presence of polyanions in amyloid deposits, the degree of specificity and the nature of the interactions involved are controversial. While attempts to identify a heparin binding consensus sequence within amyloidogenic precursors have been challenging (*7*), several studies have demonstrated the importance of electrostatic interactions in the binding of polyanions to amyloid fibrils (*21*−*24*). In particular, it has been shown that removal of

† This work was supported by grants from the Wellcome and Leverhulme Trust, from the European Commission (Research Directorates, Project HPRN-CT-2002-00241), and from the Italian MIUR (PRIN 2003025755_003 and FIRB RBAVO15B47).

* To whom correspondence should be addressed. E-mail: cmd44@cam.ac.uk. Tel: +44(0)1223763070. Fax: +44(0)1223336362.

‡ University of Cambridge.

§ Università degli Studi di Firenze.

[1] Abbreviations: AcP, human muscle acylphosphatase; ATR-FTIR, attenuated total reflection Fourier transform infrared; bzP, benzoyl phosphate; GAGs, glycosaminoglycans; HL, human lysozyme; ssDNA and dsDNA, single and double stranded DNA, respectively; TFE, 2,2,2-trifluoroethanol; ThT, thioflavin T.

10.1021/bi0610653 CCC: $33.50
Published on Web 09/19/2006

all the sulfate groups from heparin leads to a complete loss of the enhancement of Aβ peptide aggregation observed for heparin itself (*23*).

To shed further light on the various features underlying the interactions with amyloid fibrils, we have examined the binding properties of single-stranded (ss) and double-stranded (ds) DNA, ATP, heparin, and heparan sulfate, which are representative of three major nonproteinaceus biological polyanions, i.e., nucleic acids, nucleotides, and GAGs. These polyanions differ significantly from each other in terms of being highly structured (nucleic acids) or unstructured (GAGs), intracellular (nucleic acids, nucleotides) or extracellular (GAGs), in bearing different charged groups (phosphates or sulfates) and in having high (GAGs, nucleic acids) or low (nucleotides) molecular weights. The binding properties of these polyanions to preformed amyloid fibrils as well as their ability to promote protein aggregation were investigated. Two substantially different systems, both of which have been shown to form well-defined amyloid fibrils in vitro (*25*, *26*), were used: human muscle acylphosphatase (AcP), which is not linked with any pathologic condition, and human lysozyme (HL), several of whose variants are associated with a familial form of non-neuropathic amyloidosis (*27*−*29*). All the polyanions used in this study were found to bind with high affinity, but low specificity, to preformed amyloid aggregates of AcP and HL and also to increase the aggregation rate of partially unfolded AcP. Inhibition by magnesium or calcium salts of the binding and of the aggregation rate enhancement supports the idea that these interactions are primarily electrostatic in nature. Most importantly, the increase in the aggregation rate of AcP in the presence of polyanions appears to be dependent on the length and total charge of the various polyelectrolytes.

EXPERIMENTAL PROCEDURES

Materials, Protein Production, and Purification. Porcine intestinal heparin (grade I-A, molecular weight 18 000), HL, heparan sulfate from porcine intestinal mucosa (molecular weight 7500), polylysine (molecular weight 70 000−150 000), AMP, ADP (sodium salts), and ATP (sodium and magnesium salts) were obtained from Sigma-Aldrich (Gillingham, U.K.); ssDNA (41 bp) was purchased from Operon (Cologne, Germany). pRSET-B plasmid DNA (2.9 kbp) was linearized by restriction endonuclease digestion with *Bam*HI (New England Biolabs, Hitchin, U.K.). The resulting dsDNA was purified with a Qiagen purification column. Expression and purification of wild-type AcP were carried out according to the procedures described previously (*30*). The cysteine at position 21 was replaced by serine in order to avoid complexities arising from the presence of a free thiol group: the resulting mutant is described here as the wild-type protein as in previous studies (*31*). Protein concentration was measured by UV absorption using ϵ_{280} values of 1.49 mL mg^{-1} cm^{-1}. For HL, 1 mg of protein has an absorbance of 2.55 at 280 nm (*32*).

HL Fibril Formation. Wild-type HL at a concentration of 0.1 mg/mL (∼7 μM) was incubated in 0.1 M citrate buffer pH 5.0, 3 M urea, at 55 °C with stirring in a Cary Eclipse spectrofluorimeter (Varian Ltd., Oxford, U.K.). The excitation wavelength was 500 nm, and changes in fluorescence emission intensity were monitored at 500 nm with slit widths of 5 nm. The presence of fibrils in the various samples was confirmed by EM. For the amorphous aggregates, 0.3 mg/mL HL was heated at 42 °C overnight in PBS and 20 mM DTT.

AcP Fibril Formation and Aggregation Kinetics. Aggregation of AcP was initiated by incubating the protein at a concentration of 0.4 mg/mL (∼35 μM) in 25% (v/v) 2,2,2-trifluoroethanol (TFE), 50 mM sodium acetate buffer, pH 5.5, 25 °C. The polyanion assay solutions were prepared by first dissolving specific quantities of DNA, AMP sodium salt, ADP sodium salt, ATP sodium salt, ATP magnesium salt, polylysine, heparin or heparan sulfate in 50% TFE, 50 mM sodium acetate, and then by adding, in each case, a volume of the resulting solution to the same volume of a solution containing AcP (0.8 mg/mL, 50 mM sodium acetate). To test the effect of salts, AcP was incubated under these conditions but in the presence of 0.1 mg/mL heparin and 100 mM $MgSO_4$ or $CaCl_2$.

Disaggregation Kinetics of AcP. After incubating AcP for 120 min under the aggregation conditions described above, the protein was diluted 5-fold with 50 mM sodium acetate buffer, 0.1 mg/mL heparin, pH 5.5 to 0.08 mg/mL, 5% TFE (v/v).

Thioflavin T (ThT) Assay. During the aggregation process, 60 μL aliquots of the sample were mixed at regular time intervals with 440 μL of 50 mM acetate buffer, pH 5.5, 25 °C, containing 25 μM ThT. During the disaggregation process, 300 μL aliquots of the sample were withdrawn at regular time intervals and mixed with 200 μL of 50 mM acetate buffer, pH 5.5, 25 °C, containing 110 μM ThT. A Cary Eclipse spectrofluorimeter (Varian Ltd., Oxford, U.K.) with excitation and emission wavelengths of 440 and 485 nm, respectively, was used to determine ThT fluorescence values. Single-exponential functions were fitted to the kinetic plots reporting the measured ThT fluorescence versus time in order to determine the apparent aggregation rate constants.

Enzymatic Activity Assay. Seven microliter aliquots of samples containing 0.4 mg/mL AcP, 50 mM sodium acetate, incubated at different heparin concentrations (0−1 mg/mL) for 1 day, were mixed with 1 mL of 0.1 M acetate buffer, pH 5.5, 25 °C, containing 3 mM bzP. The enzymatic activity of AcP was measured by a continuous spectrophotometric method, using benzoyl phosphate (bzP) as substrate as previously described (*33*). A Varian Cary 400 spectrophotometer and a wavelength of 283 nm were used to follow the real-time decrease in absorbance resulting from the bzP hydrolysis. Each point of the plot in Figure 4c refers to the slope extrapolated from the linear phase of each activity measurement (average of three experiments) against heparin concentration. To test the effect of salts, AcP was incubated under the conditions used above in the presence of 0.1 mg/mL heparin and different concentrations of magnesium or calcium acetate (0.001−100 mM), pH 5.5, 25 °C.

DNA Binding Assay. To study interactions of fibrils with ssDNA, preformed amyloid fibrils or aggregates were centrifuged and resuspended to give final solutions containing 0.35−0.7 mg/mL HL fibrils (corresponding to a monomeric concentration of 25−50 μM, respectively), 0.35−1.4 mg/mL HL amorphous aggregates (corresponding to a monomeric concentration of 25−100 μM, respectively), or 0.8 mg/mL AcP fibrillar or prefibrillar aggregates (corresponding to a monomeric concentration of 70 μM), and 0.2 (∼20 μM)

or 0.1 mg/mL (~10 μM) DNA, respectively. Following incubation for 1 h at 25 °C, the samples were centrifuged and 10 μL aliquots of the supernatants analyzed on a 2% or 0.8% agarose E-gel (Invitrogen, Paisley, U.K.). DNA was visualized through its interaction with ethidium bromide. To test the effect of salts, some samples were incubated in the presence of increasing concentration of $MgSO_4$ or $CaCl_2$ (10−360 mM).

ATP Binding Assay. HPLC pumps (LC-10AD), detector (SPD-M10AVP diode array) and controller (SCL-10A) were from Shimadzu. A Brownlee HPLC column (Perkin-Elmer) Aquapore RP-300-7UM 0.4 × 25 cm (C8 reverse phase) was used. The mobile phase was double-distilled water containing 0.1% TFA. Preformed amyloid fibrils were centrifuged and resuspended to give 100 μL final solutions containing 0.2 mg/mL HL fibrils or 0.8 mg/mL AcP fibrils and 200 μM ATP. Following incubation for 1 h at 25 °C, samples were centrifuged and 80 μL aliquots of the supernatant were analyzed by HPLC. To test the effect of salts, the remaining 20 μL aliquots together with the pellet were added to 80 μL solutions containing different concentrations of $MgSO_4$ (0.005−250 mM), incubated for 1 h, then centrifuged and 80 μL aliquots of the supernatant were analyzed by HPLC. The effective quantity of ATP released was calculated by subtracting the areas of the peaks corresponding to ATP not bound to the fibrils from the total area of ATP peak in the reference sample, and considering this quantity as the maximum ATP available for release after addition of $MgSO_4$.

Intrinsic Fluorescence. A Varian Cary Eclipse spectrofluorimeter with excitation and emission wavelengths of 230 and 344 nm, respectively, was used to record the fluorescence intensities of protein samples.

Attenuated Total Reflection Fourier Transform Infrared (ATR-FTIR) Spectroscopy. ATR-FTIR spectra were recorded using a Bruker Equinox55 spectrometer (Ettlingen, Germany) equipped with a liquid N_2-cooled MCT detector, and purged with a continuous flow of N_2 gas. A BioATRCell II accessory from Bruker was used as a sampling system. Spectra were measured at 25 °C and, for each sample, 256 interferograms were accumulated at a spectral resolution of 2 cm^{-1}. Spectra of the buffers were recorded under conditions identical to those of the protein samples and automatically subtracted from the spectra of the proteins using Bruker Protein Dynamics software. Spectra were baseline corrected and then normalized, such that the minimally occurring *y*-value was set to zero and the maximally occurring *y*-value to 2 absorbance units.

RESULTS

DNA and Amyloid Fibrils. To study the nature of the interactions of polyanions with amyloid fibrils, the ability of preformed fibrils of HL to bind to ssDNA was first tested. A solution of 0.2 mg/mL (20 μM) ssDNA (41 bases) was incubated at pH 7.0 for 1 h with 0.7 mg/mL HL fibrils (corresponding to a protein monomer concentration of ~50 μM) and then centrifuged to remove the fibrils from solution. The resulting supernatant was analyzed using an agarose gel containing ethidium bromide. The gel did not reveal any residual DNA in the supernatant, suggesting that all the ssDNA that was initially present in solution was bound to the fibrils (Figure 1a). Under the conditions of this experiment, the net charge of monomeric HL is +8 while a single molecule of ssDNA is strongly negative (−41). To explore the role of electrostatics in the binding, we repeated the experiment in the presence of concentrations of $MgSO_4$ ranging from 10 to 360 mM (Figure 1a). Interaction of these cations with ssDNA that has not been preincubated with amyloid fibrils causes rearrangements of the linear structure of ssDNA resulting in band smearing; preincubation with

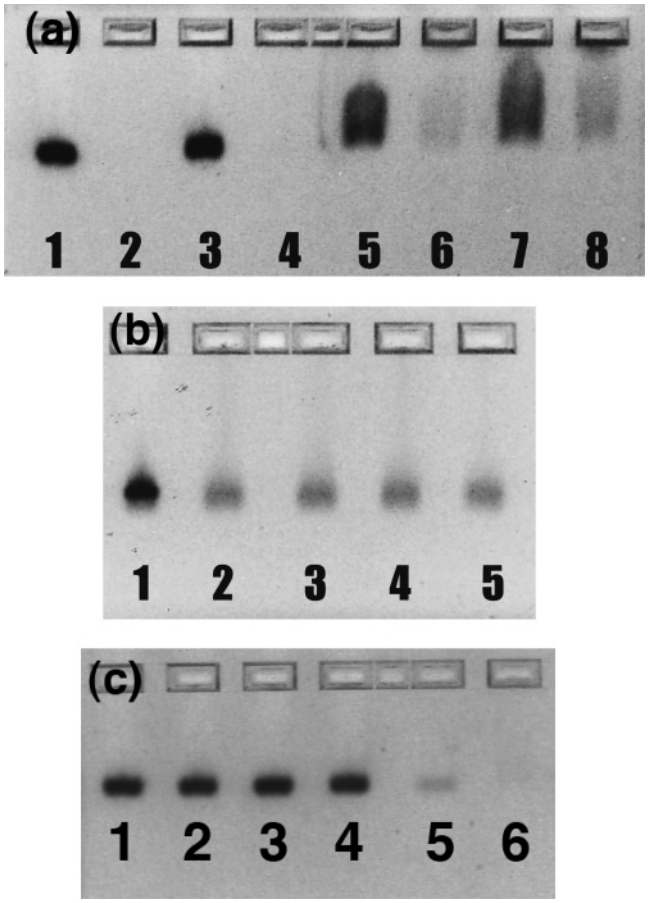

FIGURE 1: DNA and amyloid fibrils. (a) Agarose gel electrophoresis of free ssDNA present in the solution after centrifugation following incubation for 1 h with 0.7 mg/mL of preformed HL fibrils (corresponding to a monomeric concentration of ~50 μM) at different salt concentrations. Lanes: 1, ssDNA only (20 μM); 2, HL fibrils + 20 μM ssDNA (no $MgSO_4$); 3, 20 μM ssDNA only (10 mM $MgSO_4$); 4, HL fibrils + 20 μM ssDNA (10 mM $MgSO_4$); 5, 20 μM ssDNA only (250 mM $MgSO_4$); 6, HL fibrils + 20 μM ssDNA (250 mM $MgSO_4$); 7, 20 μM ssDNA only (360mM $MgSO_4$); 8, HL fibrils + 20 μM ssDNA (360 mM $MgSO_4$). (b) Agarose gel electrophoresis of free ssDNA present in the supernatant after centrifugation following incubation for 1 h with 0.8 mg/mL of preformed AcP aggregates (corresponding to a monomeric concentration of 70 μM) that were preincubated for different lengths of time. Lanes: 1, ssDNA only (10 μM); 2, AcP fibrils (2 h) + 10 μM ssDNA; 3, AcP fibrils (1 day) + 10 μM ssDNA; 4, AcP fibrils (1 week) + 10 μM ssDNA; 5, AcP fibrils (1 month) + 10 μM ssDNA. (c) Agarose gel electrophoresis of free ssDNA present in the supernatant after centrifugation following incubation for 1 h with different concentrations of preformed fibrils and amorphous aggregates of HL. Lanes: 1, ssDNA only (20 μM); 2, amorphous HL aggregates (0.35 mg/mL) + 20 μM ssDNA; 3, amorphous HL aggregates (0.7 mg/mL) + 20 μM ssDNA; 4, amorphous HL aggregates (1.4 mg/mL) + 20 μM ssDNA; 5, HL amyloid fibrils (0.35 mg/mL) + 20 μM ssDNA; 6, HL amyloid fibrils (0.7 mg/mL) + 20 μM ssDNA.

fibrils and 360 mM $MgSO_4$, however, leads to an increase in the concentration of free DNA in the supernatant, suggesting the involvement of Coulombic interactions in the binding between HL fibrils and ssDNA. $CaCl_2$ had a comparable effect to $MgSO_4$. Complete removal of DNA from solution was also observed after incubation of 0.2 mg/mL HL fibrils (corresponding to a monomeric concentration of ~15 μM) with ~2.9 kbp long linear or circular dsDNA (25 nM), suggesting that binding involves the phosphate groups rather than heterologous hydrogen bonds between the DNA bases and the fibrils.

To investigate further the specificity of the binding interactions, 0.1 mg/mL of the same ssDNA (10 μM) was incubated with 0.8 mg/mL of preformed amyloid fibrils of AcP (corresponding to a monomeric concentration of 70 μM). A reduction of ssDNA in the supernatant was found after centrifugation, a finding similar to that observed in the experiment involving HL (Figure 1b). Like HL, AcP is positively charged (+5) under the conditions used in these experiments. In this case, however, not all the ssDNA was carried down by the fibrils because the DNA binding was limited by the quantity of amyloid fibrils; at higher AcP/DNA ratios the entire population of DNA molecules was found to be associated with the fibrils (Supporting Information). To examine the importance of the morphological character of the fibrils, experiments were also carried out with prefibrillar aggregates of AcP that formed within 2 h of incubation in 25% TFE (*25*). No difference was observed in the quantity of bound ssDNA after incubation with this form of aggregated AcP compared to the more fibrillar species, implying that the binding is relatively nonspecific in character (Figure 1b). However, we do not know yet the extent of conformational differences between prefibrillar and fibrillar aggregates of AcP; although they appear morphologically different by electron microscopy, no significant changes in the content of β-sheet structure were previously observed by circular dichroism between these species (*25*). To test the binding specificity of ssDNA to amyloid aggregates, 20 μM ssDNA was incubated in the presence of increasing concentrations of preformed non-amyloid aggregates of HL, ranging from 0.35 to 1.4 mg/mL. While HL amyloid fibrils were found to bind ssDNA in a concentration dependent manner, no change was seen in the amount of free ssDNA for the amorphous aggregates (Figure 1c). In conclusion, these results suggest that the affinity of ssDNA is higher for ordered aggregates containing a high content of β-sheet structure than for less structured aggregates.

Experiments were also carried out to probe the effect of DNA on the kinetics of aggregation. The results show that as little as 0.05 mg/mL ssDNA (5 μM) can cause a very significant enhancement of the aggregation rate of AcP under appropriate conditions (Table 1), i.e., at a concentration of 0.4 mg/mL AcP (35 μM) in 25% TFE, 50 mM sodium acetate, pH 5.5, 25 °C (*25*). Aggregation of AcP can be followed by monitoring changes in the intrinsic or ThT derived fluorescence. Since DNA alone leads to an increase in ThT fluorescence intensity that is much higher than that resulting from the aggregates, the former methodology was chosen to monitor aggregation. The process of aggregation of AcP in the presence of 0.05 mg/mL ssDNA was extremely fast, being complete within the dead-time of the experiment (~1 min).

Table 1: Aggregation of AcP in the Presence of Different Polyanions

	ratio of charges (−/+)[a]	approx mol wt	k_{agg} (s^{-1})[b]
standard conditions[c]			$(7.3 \pm 0.5) \times 10^{-4}$
0.05 mg/mL ssDNA	0.91	12 500	>0.1[d]
1 mM AMP	5.5	350	$(9.9 \pm 0.5) \times 10^{-4}$
1 mM ADP	11.1	430	$(1.3 \pm 0.5) \times 10^{-3}$
1 mM ATP (~0.5 mg/mL)	16.6	510	$(1.7 \pm 0.5) \times 10^{-3}$
0.01 mg/mL heparin	0.39	18 000	$(2.2 \pm 0.5) \times 10^{-3}$
0.1 mg/mL heparin	3.9		$(1.1 \pm 0.5) \times 10^{-2}$
1 mg/mL heparin	39.4		$(2.1 \pm 0.5) \times 10^{-3}$

[a] Ratio between the total number of net charges of the various polyanions (negative) and net charges of AcP (positive). [b] The rate constant for aggregation measured as described in Experimental Procedures. [c] 0.4 mg/mL AcP, 25% TFE (v/v), 50 mM sodium acetate, pH 5.5, 25 °C. [d] A more specific value could not be determined in this case since the aggregation process was complete within the dead time of the experiment (1 min).

ATP and Amyloid Fibrils. The ability of amyloid fibrils to bind to ATP was also tested, partly because the monomeric units of nucleic acids are nucleotides, but also because this polyanion is abundant in the cytoplasm (1−10 mM), being the most important source of cellular energy. ATP (200 μM) was incubated with preformed and concentrated amyloid fibrils of HL (0.2 mg/mL, corresponding to a monomeric concentration of 15 μM) or AcP (0.8 mg/mL, corresponding to a monomeric concentration of 70 μM) for 1 h. The samples were subsequently centrifuged, and the supernatants were analyzed using HPLC. Only a very small amount of ATP (≤5%) remained in solution after centrifugation (Figure 2a,b); resuspension of the pellets in 250 mM $MgSO_4$ solutions, however, led to the complete release of ATP from the fibrils, i.e., all the ATP present in the samples was found in the supernatants after further centrifugation of the samples (Figure 2a,b). A quantitative plot of released ATP versus Mg^{2+} concentration sets the maximum concentration for release at 20−50 mM (Figure 2c). The release of ATP can be attributed to the ability of Mg^{2+} ions to compete with the positively charged fibrils for binding to ATP, suggesting that the interaction between ATP and amyloid fibrils is based on strong, but reversible, electrostatic interactions.

To investigate whether ATP has any effect on the aggregation rate of AcP, and if the negatively charged phosphate groups are involved in binding to the aggregates, AcP was incubated at a concentration of 0.4 mg/mL (35μM), in 25% TFE, 50 mM sodium acetate, pH 5.5, 25 °C in the presence of 1 mM ATP (~0.5 mg/mL), 1 mM ADP or 1 mM AMP. The process was followed by monitoring the changes in ThT fluorescence, and a single exponential function could be fitted to the time courses to obtain the apparent aggregation rate constants (Figure 3a and Table 1). A plot of rate constant versus the number of negatively charged phosphate groups in the added nucleotide shows a significant linear correlation (Figure 3b), thus highlighting the substantial contribution of electrostatic interactions to the nucleotide-induced acceleration of AcP aggregation. A control experiment carried out using the magnesium salt, rather than the sodium salt, of ATP showed no significant differences in the kinetic profile of AcP aggregation with respect to the experiments carried out in the absence of ATP. This result can be attributed to the specific ability of the

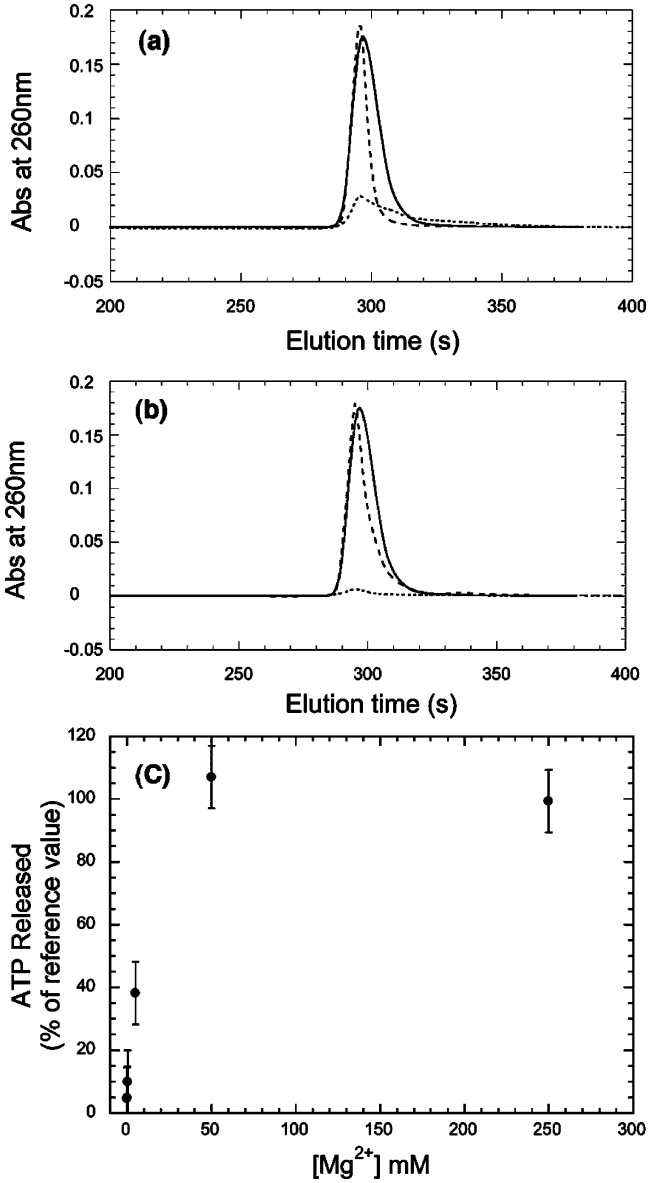

FIGURE 2: ATP and amyloid fibrils. Elution profile of free ATP present in the supernatant after centrifugation following incubation of ATP (200 μM) for 1 h with preformed HL (a) or AcP (b) fibrils at a concentration of 0.2 mg/mL (corresponding to a monomeric concentration of ~15 μM) and 0.8 mg/mL (corresponding to a monomeric concentration of 70 μM), respectively. Solid line: ATP only. Dotted line: ATP + amyloid fibrils. Dashed line: ATP released from fibrils after resuspension of the pellets in solutions of 250 mM $MgSO_4$ and further centrifugation. (c) Amount of ATP previously bound to HL fibrils and released upon addition of different concentrations of $MgSO_4$.

Mg^{2+} ion to bind tightly to ATP. No significant differences in the maximum intensity of ThT fluorescence were detected for samples incubated in the presence or absence of ATP, ADP, or AMP.

As negative control experiment, we have tested the effect of a positively charged polyelectrolyte such as polylysine on the aggregation rate of AcP. Strikingly, when the aggregation of AcP was carried out in the presence of 0.1 mg/mL polylysine, the rate of aggregation was significantly reduced (Figure 3c). This result not only suggests that polyanions promote the aggregation of positively charged proteins by compensation of electrostatic repulsion, but also shows that polycations, on the other hand, can strongly inhibit

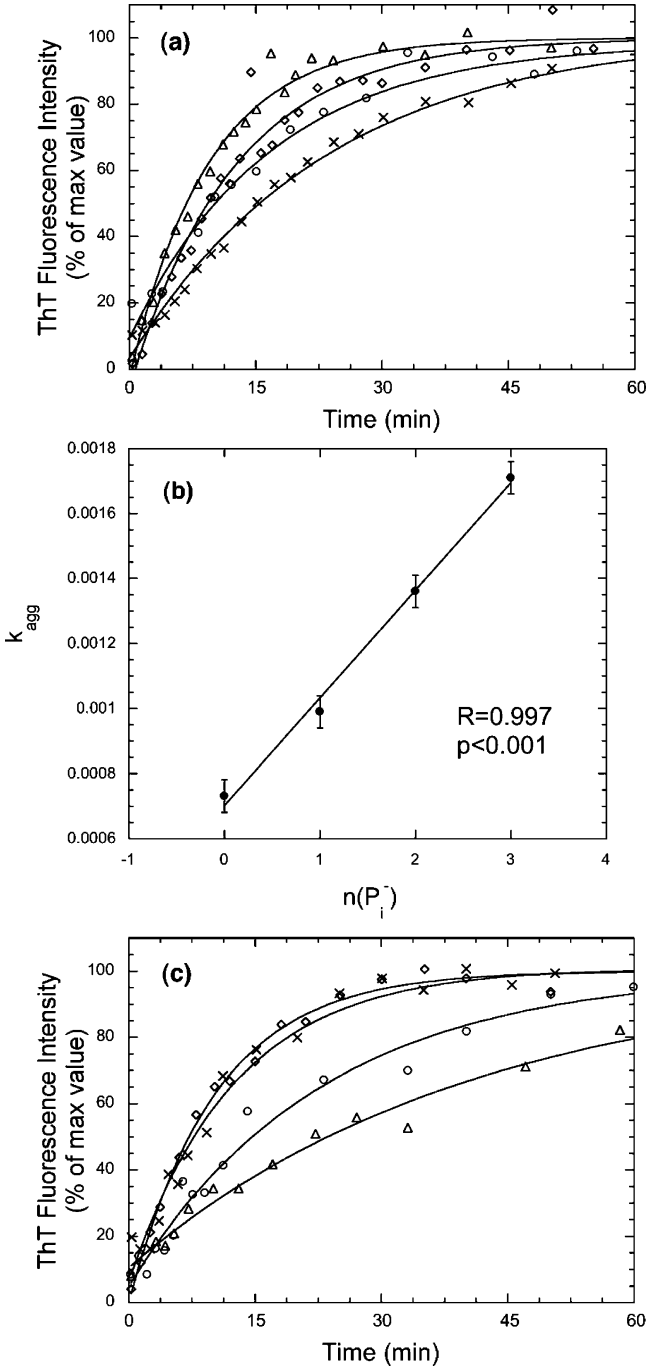

FIGURE 3: Effect of nucleotides and polylysine on the aggregation of AcP. (a, c) Aggregation of AcP monitored by ThT assay. (a) 0.4 mg/mL AcP was incubated in 25% TFE, 50 mM sodium acetate, pH 5.5, 25 °C, in the absence (crosses) or presence of 1 mM AMP (circles), ADP (diamonds), or ATP (triangles), respectively. (b) Correlation between the rate constant for AcP aggregation and the number of phosphate groups of the nucleotide added to the sample at a concentration of 1 mM; $n(P_i) = 0$ (AcP only), 1 (AcP + AMP), 2 (AcP + ADP), 3 (AcP + ATP). (c) 0.4 mg/mL AcP was incubated in 25% TFE, 50 mM sodium acetate, pH 5.5, 25 °C, in the absence (circles) or presence of 0.1 mg/mL polylysine (triangles), 1 mM ATP (diamonds) or 1 mM ATP and 0.1 mg/mL polylysine (crosses), respectively.

the aggregation of a positively charged protein. Following this result, we have tested the effect of polylysine on the enhancement in the rate of aggregation of AcP due to the presence of ATP. The aggregation of AcP was carried out in the presence of 1 mM (0.5 mg/mL) ATP with or without

the addition of 0.1 mg/mL polylysine. In this case, however, where a sum of the effects due to ATP and polylysine would have been expected, no significant change in the rate of aggregation of AcP was observed in the presence or absence of polylysine (Figure 3c). Compared to the effect caused by the presence of magnesium, polylysine appears to be less effective at decreasing the accelerating effect of ATP on the aggregation of AcP, probably because of the high intrinsic metal binding affinity of ATP for magnesium (constant affinity per mole 9554), or because, under the conditions used here, the approximate number of total positive charges for polylysine (7×10^{-4}/mL) was lower than for magnesium (2×10^{-3}/mL).

Glycosaminoglycans and Amyloid Fibrils. The effects of heparin and heparan sulfate on the aggregation behavior of AcP were explored to determine if the effects observed for DNA and ATP on positively charged amyloid fibrils are a consequence of nonspecific electrostatic interactions between polyelectrolytes or of specific binding. AcP was incubated under the standard conditions for aggregation (a concentration of 0.4 mg/mL in 25% TFE, pH 5.5, 25 °C) in the presence and absence of different concentrations of heparin or heparan sulfate, ranging from 0.01 to 1 mg/mL. Samples of AcP that had aggregated in the presence or absence of heparin were also analyzed by EM and did not reveal significant differences in morphology (Supporting Information). CD analysis also showed the typical spectrum characteristic of β-sheet structure (Supporting Information). The aggregation behavior of AcP in the presence of 0.01, 0.1, and 1 mg/mL heparin was followed by monitoring changes in ThT fluorescence intensity, and the resulting rate constants were determined from the experimental time courses of these measurements (Table 1). Heparin was found to accelerate dramatically the aggregation of AcP, with the highest rate constant obtained at a heparin concentration of 0.1 mg/mL.

Incubation of native AcP in the absence of TFE and in the presence of different concentrations of heparin results in precipitation, a phenomenon observed for many other proteins under similar circumstances (*34*). ATR-FTIR spectra recorded for the precipitated protein are similar to that of native AcP in solution in the absence of heparin, indicating that the protein retains its native structure upon binding to heparin (Figure 4a), although enzymatic activity assays show that the precipitated AcP is not catalytically active. The maximum quantity of precipitated native protein, measured from the increase of the intensity of the ATR-FTIR spectrum of the pellet and from the decrease in enzymatic activity of the supernatant after centrifugation, was at approximately 0.1 mg/mL of heparin (Figure 4b). The repeat unit of the heparin chain is generally assumed to be a pentasaccharide sequence composed of three D-glucosamines and two iduronic acids, with a molecular weight of 1400 and a net charge of −10 at neutral pH, resulting from eight sulfate groups and two carboxylate groups. A heparin concentration of 0.03 mg/mL would give approximately the same number of negative net charges as the number of net positive charges contributed by AcP, at the protein concentration and solution pH used in this experiment. Under conditions in which the native state of AcP is stable, the extent of AcP aggregation is limited by the concentration of heparin until the latter reaches 0.1 mg/mL; at higher concentrations of heparin, in which a smaller number of AcP molecules per heparin chain

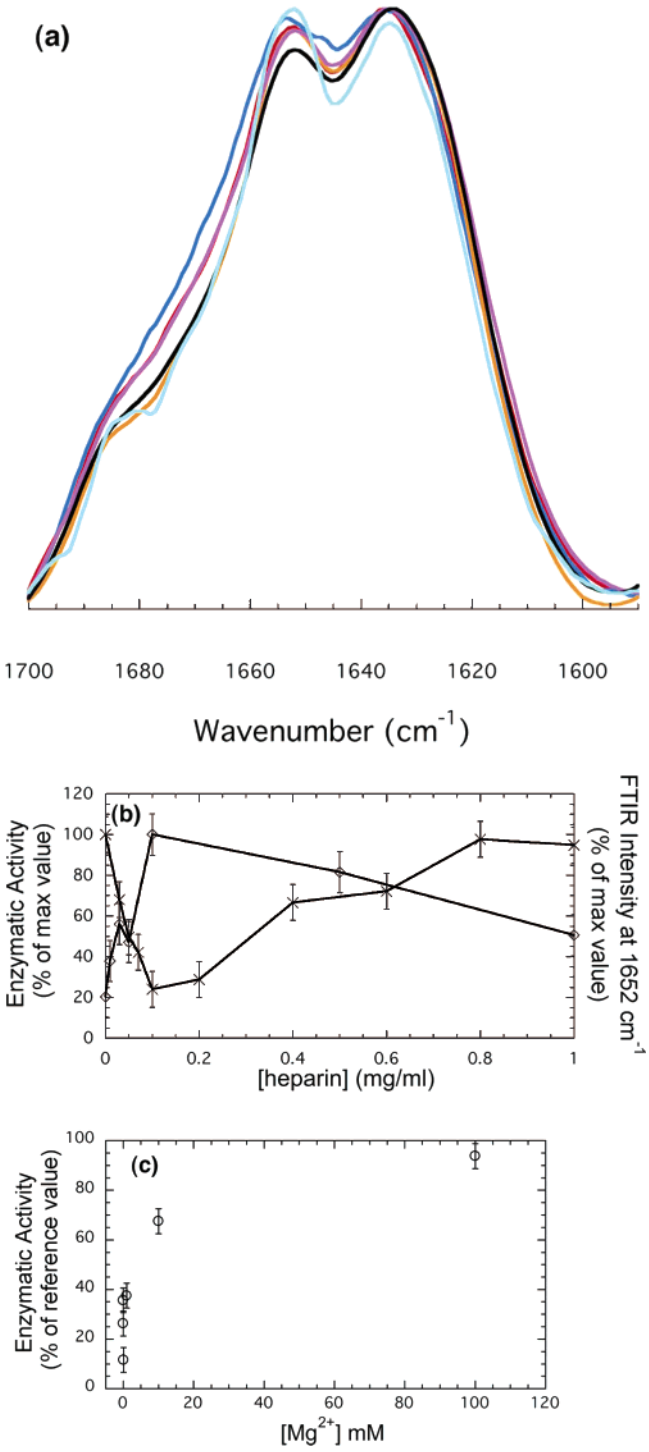

FIGURE 4: Interaction of native AcP and heparin. AcP at a concentration of 0.4 mg/mL, in 50 mM acetate buffer, pH 5.5, 25 °C, was incubated at different concentrations of heparin. (a) FTIR amide I spectra of native AcP in the presence of heparin. The blue line refers to the native state in the absence of heparin; lines in other colors indicate data for different concentrations of heparin added to native AcP: cyan, 0.01 mg/mL; purple, 0.03 mg/mL; black, 0.1 mg/mL; orange, 0.5 mg/mL; red, 1 mg/mL. Spectra were normalized to the minimum and maximum absorbance values in each experiment. (b) Changes of enzymatic activity of the supernatant (crosses) and ATR-FTIR intensity at 1652 cm^{-1} (diamonds) of the pellet of AcP recorded after incubation for 1 day followed by centrifugation. (c) Dependence of the interaction between native AcP and heparin on salt concentration: enzymatic activity of AcP in the presence of 0.1 mg/mL heparin and the indicated concentrations of magnesium acetate, pH 5.5, 25 °C.

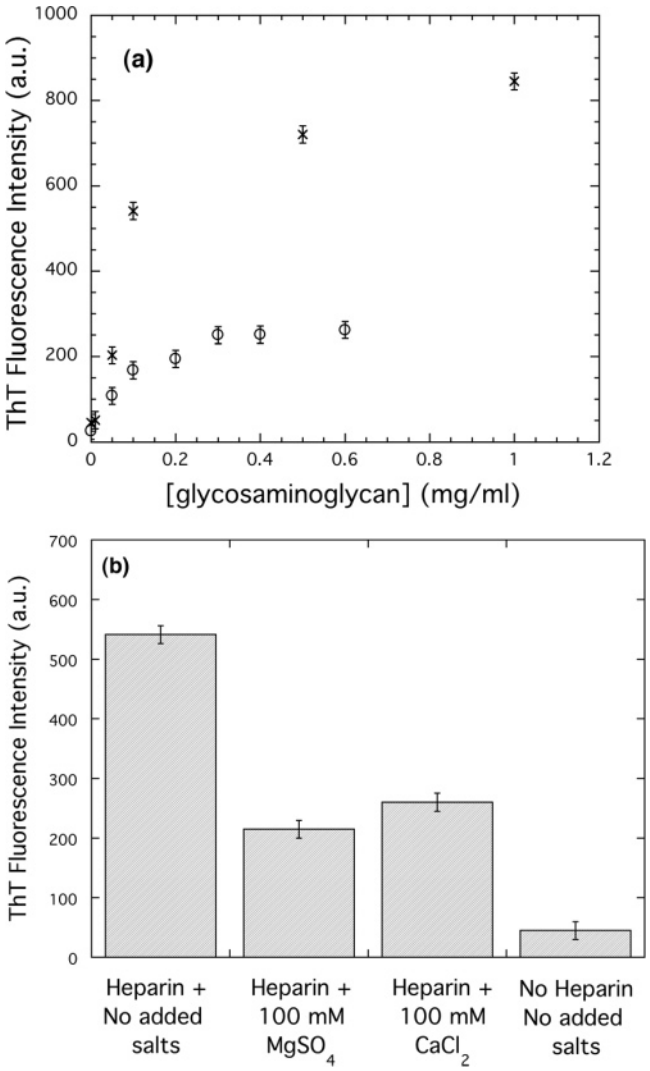

FIGURE 5: Effect of GAGs on the aggregation of AcP. (a) Changes in ThT fluorescence intensity after incubation of 0.4 mg/mL AcP in 25% TFE, 50 mM sodium acetate, pH 5.5, 25 °C, and at different concentrations of heparin (crosses) or heparan sulfate (circles), respectively. (b) Dependence of the interaction between the aggregation prone state of AcP and heparin on salt concentration: AcP was incubated in 25% TFE, 50 mM sodium acetate, pH 5.5, 25 °C, in the presence of 0.1 mg/mL heparin and 100 mM $MgSO_4$ or $CaCl_2$. The ThT fluorescence intensity is that observed at the end of the aggregation process.

is bound, the formation of aggregates is likely to be inhibited by repulsion occurring between the segments of the heparin chains not involved in the binding, thus increasing the likelihood of the dissociation of any AcP−heparin complexes. This behavior resembles the nonmonotonic ionic strength dependence of the binding constant observed for some protein−polyelectrolyte systems, where there is a peak rather than a plateau corresponding to the highest affinity (*35*, *36*).

Under conditions promoting the aggregation of AcP, the addition of increasing quantities of heparin causes a dramatic increase in the maximum ThT fluorescence intensity (Figure 5a). This increase in intensity can be attributed either to an increase in the quantity of aggregated protein or to a higher degree of order within the aggregates. Since in 25% TFE AcP is partially unfolded, and most of the molecules aggregate even in the absence of heparin (*37*), the much higher fluorescence intensity observed (∼20-fold) in the presence compared to the absence of 1 mg/mL of heparin is very likely due to a higher degree of order within the aggregates. A similar increase in intensity (4-fold), although not as marked as for heparin, was observed when heparan sulfate was added to the solution under the same aggregating conditions (Figure 5a). Heparan sulfate, whose net negative charge is lower than that of heparin (an average of −1 instead of −4 per disaccharide unit), was also found to be less effective in binding to the native state of AcP.

As observed for DNA and ATP, the presence of magnesium or calcium salts in the solution (100 mM $Mg(CH_3COO)_2$, $Ca(CH_3COO)_2$, $MgSO_4$, or $CaCl_2$) leads to a substantial decrease in the amount of native AcP bound to heparin under nonaggregating conditions (∼95% of the protein is unbound), and to a considerable reduction (∼60%) in the ThT fluorescence intensity of the aggregates under aggregating conditions (Figures 4c and 5b). However, while 100 mM magnesium salt is able to keep 95% native AcP free in solution, the same concentration is not as effective in inhibiting the binding of partially unfolded/aggregated AcP to heparin, reducing ThT intensity by only 60%. In addition, as shown previously (*37*), disassembly of the aggregates and refolding to the native state occurs when a solution containing aggregates of AcP is diluted from 25% TFE to 5% TFE, i.e., changing from unfolding to refolding conditions. However, when aggregates of AcP formed in 25% TFE in the presence of 0.1 mg/mL heparin were diluted 5-fold into a solution of 5% TFE and 0.1 mg/mL heparin, the ThT fluorescence intensity remained much higher (∼18-fold) than that which could be accounted for by the binding of heparin to native AcP. In addition, no decrease in intensity is observed over time, suggesting that heparin strongly stabilizes the aggregated state of AcP.

DISCUSSION

High Affinity, Low Specificity. The results described in this study show that aggregates of two different positively charged proteins, one of which is, and one of which is not, related to amyloid disease can bind tightly to low (ATP) or high (DNA) molecular weight polyanions, and that either prefibrillar or fibrillar aggregates of AcP bind to DNA. Interestingly, association and coprecipitation of DNA and heparin with amyloid fibrils has also recently been observed for α-synuclein, a natively unstructured protein whose aggregation is associated with Parkinson's disease (*12*, *17*). Moreover, DNA, ATP, and heparin are all able to promote the aggregation of AcP and the formation of amyloid structures. Despite the fact that no consensus sequence of the type found for serum amyloid A protein (SAA) or Aβ peptide (*7*) is present in AcP (XBBXBX, X hydrophatic, B basic), heparin appears to interact with both native and partially unfolded states of the protein. The interactions between these polyanions and proteins therefore appear to be largely nonspecific, with no obvious dependence on link to disease, type of charged groups, polyanion structure, aggregate morphology, and structure of the precursor protein. Despite of this lack of specificity, however, our results suggest a relatively high affinity between amyloid fibrils and polyanions, as shown, for example, by the fact that high salt concentrations (≥100 mM of magnesium salts) are needed to suppress the binding. It has been shown, however, that

the degree of interaction between amyloidogenic proteins and polyanions can depend on the specific features of the system concerned (*12, 13, 21, 24*).

In agreement with previous studies showing that GAGs are able to stabilize Aβ peptide fibrils (*8*) and to inhibit depolymerization of β2-microglobulin fibrils (*13*), heparin appears to stabilize AcP aggregates and maintain the protein in a misfolded conformation, as indicated by the lack of significant disassembly when the aggregates are exposed to disaggregating conditions. This result suggests that the effects observed here are general and not limited to a small number of proteins.

Electrostatic Interactions. The interactions between amyloid fibrils, formed by AcP and HL, and polyanions are suppressed or reduced in the presence of increased ionic strength, a result that suggests the dominance of electrostatic factors in the binding. That these effects are largely nonspecific is illustrated by the fact that different bivalent cations such as Mg^{2+} or Ca^{2+} have a similar inhibitory effect on binding of the polyanions. Low specificity is also evident in the case of the corresponding counterions, be they SO_4^{2-}, CH_3COO^-, or Cl^- (except for the case of ATP and Mg^{2+}, it is uncertain if cations, anions, or both in concert are responsible for the competition for interactions with amyloid fibrils and polyanions).

The strong association of polyanions with amyloid fibrils can be rationalized in a qualitative manner simply by consideration of Coulomb's law and the unfavorable entropic and enthalpic terms inherent in a polyelectrolyte molecule in comparison with an individual electrolyte. Compared to individual ions, which associate only very weakly in aqueous solutions because of their favorable entropic terms and interactions with water, the various charged groups in a polyelectrolyte are linked by covalent bonds. To decrease the electrostatic repulsions within the molecules, therefore, polyelectrolytes bind very tightly to individual counterions, and even more tightly to a polyelectrolyte of opposite charge, in this way also allowing the individual ions to equilibrate with the solvent. Although the structures of the fibrillar aggregates of AcP and HL are stabilized by noncovalent interactions, it is very likely that most of the polyelectrolyte character is retained and they can therefore be assumed to act as polycations. This conclusion explains why higher concentrations of salts are needed to displace heparin from aggregated than from monomeric native AcP. Moreover, the observed stabilization of AcP aggregates by heparin is likely to be due to compensation of the electrostatic repulsions between the protein molecules within the aggregates.

The strength of interactions between polyelectrolytes is likely to be strongly dependent on the density of charges on the molecular surfaces, a conclusion that is evident when comparing the approximate ratio between negative and positive charge concentrations ($-/+$), the molecular weights of the polyanions, and their effects on the aggregation rate of AcP (Table 1). For example, heparin and DNA (molecular weights $>10\,000$) are more effective at increasing the aggregation rate of AcP than AMP, ADP, or ATP (molecular weights $\sim 350-510$), despite the ratio of charges being higher for individual nucleotides than for DNA or heparin under the conditions used in this study. On the other hand, the net charge of the polyanion is an important factor as can be inferred by comparison of the effects of the same concentrations of AMP, ADP, and ATP on the aggregation rate of AcP (Table 1 and Figure 3b).

A number of recent studies have demonstrated that a reduction in the overall net charge of a protein enhances its rate of aggregation (*38*−*40*). Such a conclusion suggests that polyanions may promote the aggregation of positively charged proteins by compensating the electrostatic repulsions between protein monomers. Indeed, an increase in ionic strength has been found to promote fibril formation in a variety of proteins (*21, 24, 41*); interestingly, the order of effectiveness of anions in promoting aggregation of β2-microglobulin at low pH follows the electroselectivity series ($SO_4^{2-} > ClO_4^- > I^- > Cl^-$), indicating that anions facilitate assembly of positive β2-microglobulin molecules by direct binding rather than a generalized effect of ionic strength (*24*). Small polyanions such as ATP are likely to behave like individual anions and facilitate the intermolecular interactions between amyloidogenic regions of the protein molecules without affecting significantly the overall structures of the aggregates that develop. Longer polyanions such as heparin, however, appear to take a more intimate part in the formation of aggregates, not just by binding and decreasing the degree of electrostatic repulsion, but also by increasing the degree of order in the resulting structures. The observation that aggregates formed in the presence of heparin or heparan sulfate generate a much higher ThT fluorescence intensity than aggregates grown in their absence is not limited to AcP, but has also been observed for α-synuclein (*12*), β2-microglobulin (*13*), tau (*42*), and Aβ peptides (*23*).

An overall net positive charge in a protein does not appear to be a fundamental prerequisite for polyanions to influence the rate of aggregation. Proteins with a net negative charge, such as α-synuclein, aggregate more readily in the presence of polycations (*43, 44*), but, perhaps surprisingly, polyanions can also increase the rate of aggregation of these proteins (*12*). Such interactions with polyanions are likely to occur if the proteins have a global distribution of charges that is dipolar or possess specific clusters of positively charged amino acids, as in the N-terminal region of α-synuclein (*12, 36*).

Biological Relevance. The interaction of biological polyanions, such as DNA, heparin, or ATP, with amyloid aggregates appears, from the evidence described here and elsewhere, to be a general phenomenon, rather than just a feature of a small number of proteins. This phenomenon is extremely likely to contribute significantly to the promotion of amyloid fibril formation in vivo and to the stabilization of the resulting aggregates. Moreover, in the light of the discussion above concerning polyelectrolytes, aggregation of misfolded proteins in vivo might be expected to increase dramatically the strength of the electrostatic interactions of the protein molecules with free ions and, to an even greater extent, with other polyelectrolytes. Such an effect could have major consequences for a range of cellular functions. In addition to the examples considered here, GTP, RNA, tubulin, and actin are just a few other relatively abundant biological polyanions that are likely to bind to positively charged aggregates and thus be compromised in their function. Similarly, negatively charged aggregates could easily sequester important polycations such as histones and polyamines. Under normal conditions, cellular polyanions are usually found complexed with other specific polyelec-

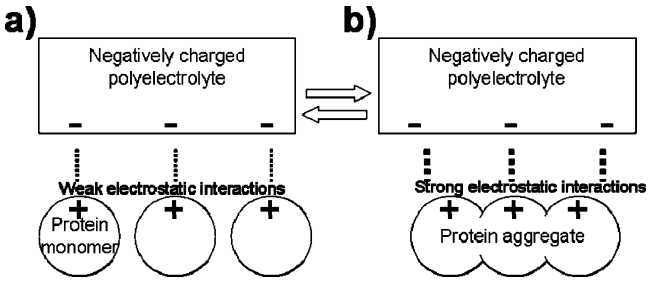

FIGURE 6: Schematic representation of the effects of protein aggregation on electrostatic interactions between two oppositely charged systems. Protein aggregation will constrain positively charged monomers to stay close to each other, causing a high localized electrostatic repulsion. Such repulsion will be compensated by strong interactions with negatively charged polyelectrolytes. Assuming, for example, that the rectangle is a polyanion such as heparin and the circle is a positively charged protein such as AcP, the interaction between these systems will be stronger when AcP is aggregated (b) rather than in its native state (a).

trolytes (e.g., DNA and histones) or ions (e.g., Mg^{2+} and ATP) of opposite net charge; the formation of large aggregates bearing a high net charge could, however, shift the association of at least some polyanions from their physiological target to these misfolded species (Figure 6), causing cellular dysfunction and generating more aggregates. An extremely interesting finding in the context of this discussion is that coprecipitation with polyglutamine aggregates has been found to cause a depletion of essential proteins and hence to impair cellular functions (*45*). Furthermore, a high net charge could allow aggregates to interact more effectively with the phospholipids of the plasma membrane.

Following the in vitro observation that high salt concentrations can suppress such interactions, the effect of ions in vivo may not be just to screen the charge of functional polyelectrolytes, but also simultaneously to buffer to some degree the electrostatic attractions between aggregated charged proteins and polymers with opposite charge, thus decreasing the potential of the aggregates to interact with vital molecules essential to cellular function. Clinical situations, trauma, or diseases such as diabetes or heart dysfunction can induce the imbalance of electrolyte homeostasis (*46*) that could be indirectly reflected in protein aggregation. Within the context of neurodegeneration, it is interesting to note that trauma arising, for example, from a head injury can induce the depletion of magnesium in brain tissue (*47*) and that aging is responsible for deficits in both calcium and magnesium ions (*48*, *49*).

Finally, and highly speculatively, in the light of recent findings on the prebiotic role of clay in catalyzing the polymerization of RNA from activated ribonucleotides (*50*, *51*), and from the observation that amyloid fibrils could represent a primordial polypeptide conformation, amyloid aggregates could as well have assisted the polymerization of nucleotides (*52*). The strong interactions of amyloid fibrils with nucleotides and DNA found here supports this idea, where the twisted morphology of the fibrils could potentially work as a more effective and more specific template than clay. Translation of RNA into proteins with a high tendency to aggregate could thus have accelerated the process of synthesis of new polynucleotides, facilitating the coevolution of proteins and nucleic acids.

In summary, whether or not the cytotoxic effect of amyloid aggregates results from their interactions with biological polyanions, or whether fibrillar amyloid structures could have had a role in the origin of life, the results presented here emphasize that such interactions can be highly significant in modulating the functions of living systems. Thus, for example, protein aggregation can be modulated generically by electrostatic interactions involving nonproteinaceous polyelectrolytes, and the decreasing ability to regulate ion homeostasis with increasing age could be one of the many factors that are responsible for the late onset of diseases related to protein misfolding.

ACKNOWLEDGMENT

We thank Donatella Degl'Innocenti for technical support.

SUPPORTING INFORMATION AVAILABLE

Agarose gel electrophoresis of free ssDNA present in the supernatant after centrifugation following incubation for 1 h with 1.2 mg/mL of preformed AcP fibrils (Supp Figure 1); EM pictures of 0.4 mg/mL AcP in 25% TFE, 50 mM sodium acetate, pH 5.5, 25 °C, after 2 h incubation in the absence (a) or presence (b) of 0.1 mg/mL heparin (Supp Figure 2); CD spectrum of 0.4 mg/mL AcP in 25% TFE, 50 mM sodium acetate, pH 5.5, 25 °C, after 2 h incubation in the presence of 0.1 mg/mL heparin (Supp Figure 3). This material is available free of charge via the Internet at http://pubs.acs.org.

REFERENCES

1. Serpell, L. C., Sunde, M., and Blake, C. C. (1997) The molecular basis of amyloidosis, *Cell. Mol. Life Sci. 53*, 871−87.
2. Dobson, C. M. (2003) Protein folding and misfolding, *Nature 426*, 884−90.
3. Selkoe, D. J. (2003) Folding proteins in fatal ways, *Nature 426*, 900−4.
4. Friedereich, N., and Kekule, A. (1859) Zur amyloifrage, *Arch. Pathol. Physiol. Klin. Med. 16*, 50−65.
5. Diaz-Nido, J., Wandosell, F., and Avila, J. (2002) Glycosaminoglycans and beta-amyloid, prion and tau peptides in neurodegenerative diseases, *Peptides 23*, 1323−32.
6. van Horssen, J., Wesseling, P., van den Heuvel, L. P., de Waal, R. M., and Verbeek, M. M. (2003) Heparan sulphate proteoglycans in Alzheimer's disease and amyloid-related disorders, *Lancet Neurol. 2*, 482−92.
7. Ancsin, J. B. (2003) Amyloidogenesis: historical and modern observations point to heparan sulfate proteoglycans as a major culprit, *Amyloid 10*, 67−79.
8. Castillo, G. M., Ngo, C., Cummings, J., Wight, T. N., and Snow, A. D. (1997) Perlecan binds to the beta-amyloid proteins (A beta) of Alzheimer's disease, accelerates A beta fibril formation, and maintains A beta fibril stability, *J. Neurochem. 69*, 2452−65.
9. McLaurin, J., Franklin, T., Zhang, X., Deng, J., and Fraser, P. E. (1999) Interactions of Alzheimer amyloid-beta peptides with glycosaminoglycans effects on fibril nucleation and growth, *Eur. J. Biochem. 266*, 1101−10.
10. Goedert, M., Jakes, R., Spillantini, M. G., Hasegawa, M., Smith, M. J., and Crowther, R. A. (1996) Assembly of microtubule-associated protein tau into Alzheimer-like filaments induced by sulphated glycosaminoglycans, *Nature 383*, 550−3.
11. Hasegawa, M., Crowther, R. A., Jakes, R., and Goedert, M. (1997) Alzheimer-like changes in microtubule-associated protein Tau induced by sulfated glycosaminoglycans. Inhibition of microtubule binding, stimulation of phosphorylation, and filament assembly depend on the degree of sulfation, *J. Biol. Chem. 272*, 33118−24.

12. Cohlberg, J. A., Li, J., Uversky, V. N., and Fink, A. L. (2002) Heparin and other glycosaminoglycans stimulate the formation of amyloid fibrils from alpha-synuclein in vitro, *Biochemistry 41*, 1502−11.
13. Yamaguchi, I., Suda, H., Tsuzuike, N., Seto, K., Seki, M., Yamaguchi, Y., Hasegawa, K., Takahashi, N., Yamamoto, S., Gejyo, F., and Naiki, H. (2003) Glycosaminoglycan and proteoglycan inhibit the depolymerization of beta2-microglobulin amyloid fibrils in vitro, *Kidney Int. 64*, 1080−8.
14. Ginsberg, S. D., Galvin, J. E., Chiu, T. S., Lee, V. M., Masliah, E., and Trojanowski, J. Q. (1998) RNA sequestration to pathological lesions of neurodegenerative diseases, *Acta Neuropathol. 96*, 487−94.
15. Kampers, T., Friedhoff, P., Biernat, J., Mandelkow, E. M., and Mandelkow, E. (1996) RNA stimulates aggregation of microtubule-associated protein tau into Alzheimer-like paired helical filaments, *FEBS Lett. 399*, 344−9.
16. Deleault, N. R., Lucassen, R. W., and Supattapone, S. (2003) RNA molecules stimulate prion protein conversion, *Nature 425*, 717−20.
17. Cherny, D., Hoyer, W., Subramaniam, V., and Jovin, T. M. (2004) Double-stranded DNA stimulates the fibrillation of alpha-synuclein in vitro and is associated with the mature fibrils: an electron microscopy study, *J. Mol. Biol. 344*, 929−38.
18. Cherny, I., Rockah, L., Levy-Nissenbaum, O., Gophna, U., Ron, E. Z., and Gazit, E. (2005) The formation of Escherichia coli curli amyloid fibrils is mediated by prion-like peptide repeats, *J. Mol. Biol. 352*, 245−52.
19. Exley, C. (1997) ATP-promoted amyloidosis of an amyloid beta peptide, *NeuroReport 8*, 3411−4.
20. Exley, C., and Korchazhkina, O. V. (2001) Promotion of formation of amyloid fibrils by aluminium adenosine triphosphate (AlATP), *J. Inorg. Biochem. 84*, 215−24.
21. Fraser, P. E., Nguyen, J. T., Chin, D. T., and Kirschner, D. A. (1992) Effects of sulfate ions on Alzheimer beta/A4 peptide assemblies: implications for amyloid fibril-proteoglycan interactions, *J. Neurochem. 59*, 1531−40.
22. Castillo, G. M., Cummings, J. A., Yang, W., Judge, M. E., Sheardown, M. J., Rimvall, K., Hansen, J. B., and Snow, A. D. (1998) Sulfate content and specific glycosaminoglycan backbone of perlecan are critical for perlecan's enhancement of islet amyloid polypeptide (amylin) fibril formation, *Diabetes 47*, 612−20.
23. Castillo, G. M., Lukito, W., Wight, T. N., and Snow, A. D. (1999) The sulfate moieties of glycosaminoglycans are critical for the enhancement of beta-amyloid protein fibril formation, *J. Neurochem. 72*, 1681−7.
24. Raman, B., Chatani, E., Kihara, M., Ban, T., Sakai, M., Hasegawa, K., Naiki, H., Rao Ch, M., and Goto, Y. (2005) Critical balance of electrostatic and hydrophobic interactions is required for beta 2-microglobulin amyloid fibril growth and stability, *Biochemistry 44*, 1288−99.
25. Chiti, F., Webster, P., Taddei, N., Clark, A., Stefani, M., Ramponi, G., and Dobson, C. M. (1999) Designing conditions for in vitro formation of amyloid protofilaments and fibrils, *Proc. Natl. Acad. Sci. U.S.A. 96*, 3590−4.
26. Morozova-Roche, L. A., Zurdo, J., Spencer, A., Noppe, W., Receveur, V., Archer, D. B., Joniau, M., and Dobson, C. M. (2000) Amyloid fibril formation and seeding by wild-type human lysozyme and its disease-related mutational variants, *J. Struct. Biol. 130*, 339−51.
27. Pepys, M. B., Hawkins, P. N., Booth, D. R., Vigushin, D. M., Tennent, G. A., Soutar, A. K., Totty, N., Nguyen, O., Blake, C. C., Terry, C. J., et al. (1993) Human lysozyme gene mutations cause hereditary systemic amyloidosis, *Nature 362*, 553−7.
28. Valleix, S., Drunat, S., Philit, J. B., Adoue, D., Piette, J. C., Droz, D., MacGregor, B., Canet, D., Delpech, M., and Grateau, G. (2002) Hereditary renal amyloidosis caused by a new variant lysozyme W64R in a French family, *Kidney Int. 61*, 907−12.
29. Yazaki, M., Farrell, S. A., and Benson, M. D. (2003) A novel lysozyme mutation Phe57Ile associated with hereditary renal amyloidosis, *Kidney Int. 63*, 1652−7.
30. Taddei, N., Stefani, M., Magherini, F., Chiti, F., Modesti, A., Raugei, G., and Ramponi, G. (1996) Looking for residues involved in the muscle acylphosphatase catalytic mechanism and structural stabilization: role of Asn41, Thr42, and Thr46, *Biochemistry 35*, 7077−83.
31. van Nuland, N. A., Chiti, F., Taddei, N., Raugei, G., Ramponi, G., and Dobson, C. M. (1998) Slow folding of muscle acylphosphatase in the absence of intermediates, *J. Mol. Biol. 283*, 883−91.
32. Booth, D. R., Sunde, M., Bellotti, V., Robinson, C. V., Hutchinson, W. L., Fraser, P. E., Hawkins, P. N., Dobson, C. M., Radford, S. E., Blake, C. C., and Pepys, M. B. (1997) Instability, unfolding and aggregation of human lysozyme variants underlying amyloid fibrillogenesis, *Nature 385*, 787−93.
33. Ramponi, G., Treves, C., and Guerritore, A. A. (1966) Aromatic acyl phosphates as substrates of acyl phosphatase, *Arch. Biochem. Biophys. 115*, 129−35.
34. Jones, L. S., Yazzie, B., and Middaugh, C. R. (2004) Polyanions and the proteome, *Mol. Cell. Proteomics 3*, 746−69.
35. Moss, J. M., Van Damme, M. P., Murphy, W. H., and Preston, B. N. (1997) Dependence of salt concentration on glycosaminoglycan-lysozyme interactions in cartilage, *Arch. Biochem. Biophys. 348*, 49−55.
36. Seyrek, E., Dubin, P. L., Tribet, C., and Gamble, E. A. (2003) Ionic strength dependence of protein-polyelectrolyte interactions, *Biomacromolecules 4*, 273−82.
37. Calamai, M., Canale, C., Relini, A., Stefani, M., Chiti, F., and Dobson, C. M. (2005) Reversal of protein aggregation provides evidence for multiple aggregated States, *J. Mol. Biol. 346*, 603−16.
38. Chiti, F., Calamai, M., Taddei, N., Stefani, M., Ramponi, G., and Dobson, C. M. (2002) Studies of the aggregation of mutant proteins in vitro provide insights into the genetics of amyloid diseases, *Proc. Natl. Acad. Sci. U.S.A. 99* (Suppl. 4), 16419−26.
39. Fandrich, M., and Dobson, C. M. (2002) The behaviour of polyamino acids reveals an inverse side chain effect in amyloid structure formation, *EMBO J. 21*, 5682−90.
40. Calamai, M., Taddei, N., Stefani, M., Ramponi, G., and Chiti, F. (2003) Relative influence of hydrophobicity and net charge in the aggregation of two homologous proteins, *Biochemistry 42*, 15078−83.
41. Zurdo, J., Guijarro, J. I., Jimenez, J. L., Saibil, H. R., and Dobson, C. M. (2001) Dependence on solution conditions of aggregation and amyloid formation by an SH3 domain, *J. Mol. Biol. 311*, 325−40.
42. Friedhoff, P., Schneider, A., Mandelkow, E. M., and Mandelkow, E. (1998) Rapid assembly of Alzheimer-like paired helical filaments from microtubule-associated protein tau monitored by fluorescence in solution, *Biochemistry 37*, 10223−30.
43. Goers, J., Uversky, V. N., and Fink, A. L. (2003) Polycation-induced oligomerization and accelerated fibrillation of human alpha-synuclein in vitro, *Protein Sci. 12*, 702−7.
44. Antony, T., Hoyer, W., Cherny, D., Heim, G., Jovin, T. M., and Subramaniam, V. (2003) Cellular polyamines promote the aggregation of alpha-synuclein, *J. Biol. Chem. 278*, 3235−40.
45. Nucifora, F. C., Jr., Sasaki, M., Peters, M. F., Huang, H., Cooper, J. K., Yamada, M., Takahashi, H., Tsuji, S., Troncoso, J., Dawson, V. L., Dawson, T. M., and Ross, C. A. (2001) Interference by huntingtin and atrophin-1 with cbp-mediated transcription leading to cellular toxicity, *Science 291*, 2423−8.
46. Weglicki, W., Quamme, G., Tucker, K., Haigney, M., and Resnick, L. (2005) Potassium, magnesium, and electrolyte imbalance and complications in disease management, *Clin. Exp. Hypertens. 27*, 95−112.
47. Vink, R. (1991) Magnesium and brain trauma, *Magnesium Trace Elem. 10*, 1−10.
48. Durlach, J., Durlach, V., Bac, P., Rayssiguier, Y., Bara, M., and Guiet-Bara, A. (1993) Magnesium and ageing. II. Clinical data: aetiological mechanisms and pathophysiological consequences of magnesium deficit in the elderly, *Magnesium Res. 6*, 379−94.
49. Toescu, E. C., Verkhratsky, A., and Landfield, P. W. (2004) Ca2+ regulation and gene expression in normal brain aging, *Trends Neurosci. 27*, 614−20.
50. Ferris, J. P., and Ertem, G. (1992) Oligomerization of ribonucleotides on montmorillonite: reaction of the 5′-phosphorimidazolide of adenosine, *Science 257*, 1387−9.
51. Hanczyc, M. M., Fujikawa, S. M., and Szostak, J. W. (2003) Experimental models of primitive cellular compartments: encapsulation, growth, and division, *Science 302*, 618−22.
52. Dale, T. (2006) Protein and nucleic acid together: a mechanism for the emergence of biological selection, *J. Theor. Biol. 240*, 337−42.

BI0610653